# A small surface hydrophobic stripe in the coiled-coil domain of type I keratins mediates tetramer stability

Kelsie M. Bernot, Chang-Hun Lee, and Pierre A. Coulombe

Department of Biological Chemistry and Department of Dermatology, Johns Hopkins University School of Medicine, Baltimore, MD 21205

Intermediate filaments (IFs) are fibrous polymers encoded by a large family of differentially expressed genes that provide crucial structural support in the cytoplasm and nucleus in higher eukaryotes. The mechanisms involved in bringing together ~16 elongated coiled-coil dimers to form an IF are poorly defined. Available evidence suggests that tetramer subunits play a key role during IF assembly and regulation. Through molecular modeling and site-directed mutagenesis, we document a hitherto unnoticed hydrophobic stripe exposed at the surface of coiled-coil keratin heterodimers that contributes to the extraordinary stability of heterotetramers. The inability of K16 to form urea-stable tetramers in vitro correlates with an increase in its turnover rate in vivo. The data presented support a specific conformation for the assembly competent IF tetramer, provide a molecular basis for their differential stability in vitro, and point to the physiological relevance associated with this property in vivo.

## Introduction

Intermediate filaments (IFs) are flexible intracellular fibrous polymers that provide resilience to the cells in which they are expressed (Fuchs and Cleveland, 1998; Omary et al., 2004). The structural support function of IFs is made possible by their unique ability to sustain relatively large deformations without breaking (Janmey, 1991; Yamada et al., 2002). Loss of this function through inherited mutations underlies a large variety of rare diseases in which affected cells and tissues are often fragile and cannot sustain mechanical stress (Omary et al., 2004). Additionally, IFs can also modulate the response to chemical stress, pro-apoptotic, and other signals, a newly defined function that involves regulated interactions with signaling effectors (Coulombe and Wong, 2004).

The human genome contains at least 67 distinct genes encoding proteins able to self-polymerize into 10-12-nm-wide IFs that are regulated in a tissue-, cell type–, and differentiation-specific fashion (Hesse et al., 2001). All IF proteins ($M_r$ 40–240 kD) share a tripartite domain organization consisting of a central α-helical "rod" flanked by nonhelical head and tail domains. In cytoplasmic IF proteins, the rod domain is 310 aa residues long and features long-range heptad repeats $(abcdefg)_n$ in which amino acid residues located in the first a and fourth d positions are hydrophobic or apolar, leading to the "knob and hole" packing of two α-helices into a stable coiled-coil dimer (Crick, 1952; Cohen and Parry, 1990). The heptad repeats are interrupted by short linker sequences at three conserved locations, segmenting the rod domain into coils 1A, 1B, 2A, and 2B (35, 101, 19, and 121 resides long, respectively; Parry and Steinert, 1999). The head and tail domains exhibit variable primary and secondary structure and are substrates for phosphorylation and other modifications that regulate IF polymer assembly, dynamics, and interactions with other proteins (Coulombe and Omary, 2002).

Resolving the high resolution structure of F-actin and microtubule fibrous polymers has catapulted these research fields to new heights. Such a detailed understanding is lacking for IFs, owing to the elongated shape and polymerization-prone nature of their constituent proteins, and structural polymorphism (Strelkov et al., 2001). Scanning transmission electron microscopy has shown that on average the IF polymer backbone consists of 16 coiled-coil dimers in cross section (Herrmann et al., 1999). Dimers are structurally elongated (46-nm length; 2–3-nm width; Quinlan et al., 1984) and polar, because of the parallel and in-register alignment of α-helices. Packing 16 dimers into a smooth surfaced, 10–12-nm filament represents a tour de force that remains poorly understood. For cytoplasmic IFs, dimers interact along their lateral surfaces with an antiparallel orientation to form apolar tetramers. In vitro, further lateral interactions between tetramers yield unit length filaments (ULFs, 16-nm width; 60-nm length), which then anneal and compact to give rise to mature IFs (Strelkov et al., 2003). Beyond dimer formation, the interactions presiding over the polymerization of IF proteins are less understood.

Correspondence to Pierre A. Coulombe: coulombe@jhmi.edu

Abbreviations used in this paper: ANS, 8-anilino-1-naphthalenesulfonic acid; $BS^3$, *Bis*(sulfosuccinimidyl)suberate; EPR, electron paramagnetic resonance; IF, intermediate filament; K, keratin.


The Journal of Cell Biology, Vol. 168, No. 6, March 14, 2005 965–974
http://www.jcb.org/cgi/doi/10.1083/jcb.200408116

Tetramers correspond to the oligomeric state of cytoplasmic IF subunits in the soluble pool in vivo (Soellner et al., 1985; Chou et al., 1993), and represent the major subunit that exists below the critical concentration for assembly in vitro (~40 μg/ml; Steinert, 1991). Through biophysical techniques, modeling, and biochemical studies, several alignment modes of the two antiparallel dimers within a tetramer have been suggested (Herrmann and Aebi, 1998). The two favored models for the assembly competent tetramer subunit consist of an antiparallel overlap in which either the 1B or the 2B coiled-coil domains of participating dimers are facing one another (designated $A_{11}$ and $A_{22}$, respectively; Geisler et al., 1992; Steinert et al., 1993a,b,c; Mucke et al., 2004). Resolving this issue is crucial for furthering our understanding of the assembly, structure, and regulation of IFs in vivo.

Keratin polymerization is initiated through the formation of heterodimers involving types I and II IF proteins. We previously reported that unlike other type I keratins to which it is highly related in primary structure, including K14 and K17, human keratin 16 (hK16) cannot form urea-stable heterotetramers with various type II partners (Paladini et al., 1996). This property is conferred by a single amino acid, proline 188 (Pro 188), occurring in a "d" position of a heptad repeat within subdomain 1B (Wawersik et al., 1997), which is occupied by hydrophobic amino acids (e.g., Val, Ile) in hK14, hK17, and several other human type I keratins. Surprisingly, the corresponding position is occupied by a Phe residue in the mouse orthologue, raising doubts as to its significance in human K16 (Porter et al., 1998). While characterizing the tetramer-forming properties of mK16, we uncovered a hitherto unnoticed hydrophobic stripe exposed on the surface of type I keratins, in a region encompassing Pro188 in human K16, that accounts for the unusual stability of keratin heterotetramers in vitro. We also show that mK16 protein turns over faster in the absence of its polymerization partner mK6 in keratinocytes in primary cultures, correlating tetramer stability in vitro with keratin turnover rate in vivo. We discuss the implication of our results for keratin tetramer structure and keratin regulation.

## Results

### Like its human orthologue, mouse K16 forms unstable tetramers with type II partner K6

We compared the ability of mK16 to form stable heterotetramers in vitro to that of hK16 and related type I keratins, hK14 and mK17. Purified types I and II keratins were mixed in the presence of 6.5 M urea and low salt and subjected to an anion exchange chromatography assay that resolves monomers, heterodimers, and heterotetramers (Wawersik et al., 1997). Whereas hK14/mK6 and mK17/mK6 elute largely as heterotetramers, both hK16/mK6 and mK16/mK6 elute primarily as monomers and heterodimers (Fig. 1 a). Complexes containing mouse or human K6 paralogues and K17 display identical properties in this assay (not depicted), establishing that behavior in this assay is not dictated by the species of origin. Purified heterotypic complexes were subjected to cross-linking of lysine side chains with *Bis*(sulfosuccinimidyl)suberate ($BS^3$), followed by electrophoretic separation of products via SDS-PAGE. Cross-linked hK14/mK6 and mK17/mK6 migrated predominantly as tetramers (>40% tetramers, <35% dimers), whereas hK16- and mK16-containing complexes migrated predominantly as dimers (>50%) with a small amount of tetramers (<20%; Fig. 1, b and c). K14, K17, and K16 have comparable numbers of lysine residues (23, 22, and 19, respectively), such that side chain availability likely did not influence cross-linking outcome.

The tetramer-destabilizing Pro188 is located in the first third of subdomain 1B in hK16 protein. We created chimeric cDNA constructs in which the coding sequences for the 1B subdomains in mK16 and mK17 were swapped, and found that again this region of the rod included the determinants underlying this property (Fig. S1, available at http://www.jcb.org/cgi/content/full/jcb.200408116/DC1). Altogether these data show that the property of forming urea-unstable heterotetramers is conserved owing to distinct biochemical determinants within subdomain 1B of human and mouse K16 proteins.

Given that the previous experiments were performed on recombinant protein, we sought to validate these findings in vivo. We solubilized cultured mouse primary keratinocytes in either 8 M or 6 M urea and separated the lysate on a blue native acrylamide gel, which resolves protein complexes in their native form according to mass. Western blotting of the resolved keratinocyte lysate revealed that K16-containing complexes were smaller than complexes containing the related type I keratins K14 or K17 (Fig. 1 d). Aside from monomers, all bands contain both types I and II keratins (K6 shown, K5 not shown). In another experiment, primary keratinocyte total protein lysates were separated by anion exchange chromatography as in Fig. 1 a. Here, K16 eluted predominantly in the type I monomer and heterodimer peaks, whereas K14 eluted predominantly in the heterotetramer peak (unpublished data). Together, these results suggest that native keratins present in total protein extracts prepared from cells in primary culture behave similarly to purified recombinant proteins.

### Type I keratins exhibit a hydrophobic stripe at the surface of coiled-coil heterodimers

Inspection of the 1B subdomain sequence in mK16 does not reveal obvious amino acid candidates likely to disrupt an α-helix and thus explain its inability to form urea-stable tetramers, unlike the prediction for Pro188 in hK16 (Wawersik et al., 1997). We applied structural modeling with the aim of identifying features that would be unique to subdomain 1B in mK16, relative to other type I keratins. We used the structure of cortexillin I as a template for modeling (PDB 1D7M; Burkhard et al., 2000) as done before (Briki et al., 2002; Hess et al., 2002), given that it consists of a 18-heptad repeat-long, uninterrupted, coiled-coil-forming domain. After aligning the target and cortexillin I sequences with ClustalX (Thompson et al., 1997), homology model building was performed using default parameters of Modeller6 (Sali and Blundell, 1993). We created several models of the in-register, parallel 1B domain of vimentin and vari-

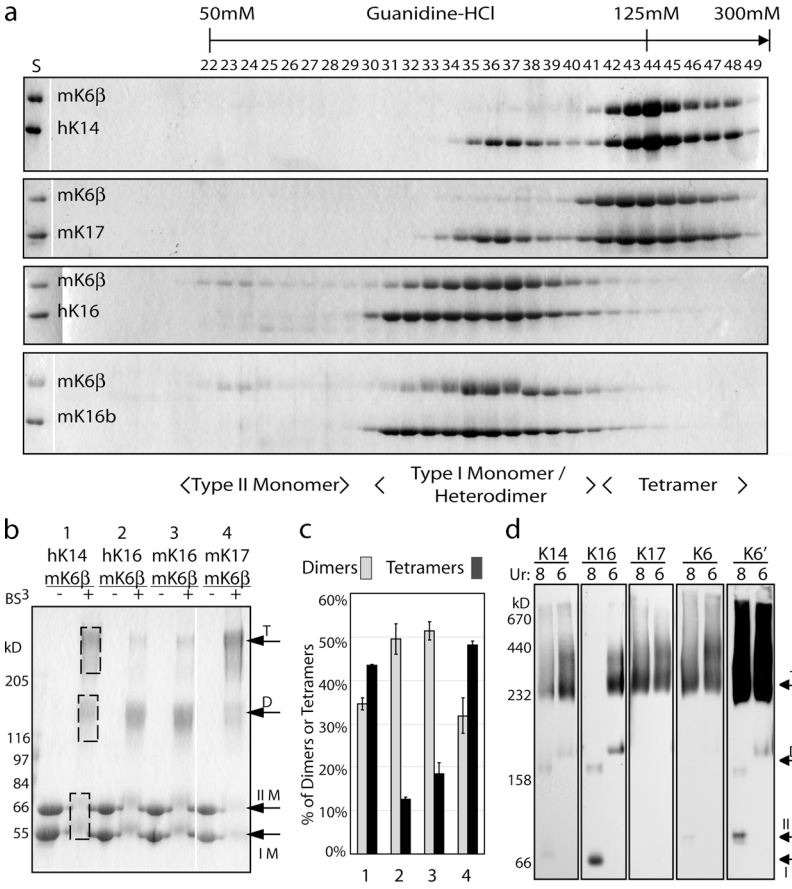


Figure 1. **Mouse and human keratin 16 form unstable tetramers with type II K6.** (a) Various purified type I keratins (human K14, mouse K17, human K16, mouse K16) were individually mixed with the mouse type II keratin K6β in a 55:45 M ratio, applied to a Mono Q anion-exchange chromatography column, and eluted with a gradient of guanidine-HCl. Fractions were analyzed by SDS-PAGE. Monomeric type II keratins elute first, followed by monomeric type I keratins and heterodimers of type I and II keratins, and finally heterotetramers of type I and II keratins (Wawersik et al., 1997). White lines indicate that intervening lanes have been spliced out. (b) Type I–type II heterotypic complexes (see panel a) were chemically cross-linked with $BS^3$. Cross-linked products (4 μg proteins) were resolved on a 4–16% gradient SDS-PAGE and stained with Coomassie blue. Although individual keratins do not cross-link under these conditions (not depicted; Coulombe and Fuchs, 1990), the type I/type II mixes cross-link as oligomers. The migration standards are indicated at left, and oligomeric complex positions of tetramer (T), dimer (D) type II (II M) and type I (I M) monomers are indicated on the right. Dotted boxes indicate region quantitated in c. The presence of multiple bands for each of the cross-linked heterodimer and heterotetramer products corresponds to distinct intramolecular cross-links. For each combination tested, antibodies to types I and II keratins react with all of these bands (not depicted), reflecting their heterotypic character. K14, K17, and K16 have comparable numbers of lysine residues (23, 22, and 19, respectively), such that side chain availability likely did not influence cross-linking outcome. There is excellent concordance between the chromatography and chemical cross-linking assays. White lines indicate that intervening lanes have been spliced out. (c) Densitometry was performed on the cross-linked products in b and in replicate experiments. The intensities of monomer, dimer, and tetramer in each lane were summed to 100%, and the percentages of tetramers (black box) and dimers (gray box) were graphed (mean ± SEM). (d) Cultured mouse primary keratinocytes were lysed with 8 M or 6 M urea, mixed with Coomassie G250 dye and separated on a blue native gel (5–13% acrylamide without SDS). Western blotting was performed after transfer to membrane and revealed monomer, dimer, and tetramer complexes of the various native keratins. The approximate migration of various recombinant proteins is indicated to the right; however, these marks should not be considered an exact molecular mass. Although a general calibration curve can be calculated for blue native gels, the apparent mass of a specific complex can vary up to 20% due to different solubilization conditions and post-translational modifications (Schagger, 2001). This explanation may also account for the difference in migration of the dimer band in 8 M versus 6 M urea. Alternatively, there may be a keratin binding protein present in 6 M urea that is dissociated in 8 M urea. Note that two different exposures are shown for K6. The darker exposure (K6′) shows that K6 is present in both monomer and heterodimer bands in 8 M urea.

ous keratin pairs. All models aligned well with the overall geometry of cortexillin I and yielded satisfactory evaluations (see Materials and methods), except mK17/mK6α, which showed a slight out of range value for surface hydrophilicity.

We expected that Pro188 in hK16 would kink the α-helical backbone and create a local disturbance at surface of the dimer (Wawersik et al., 1997). Models of the hK16/K6 dimer indeed exhibited a turn in the backbone at Pro188; however, the α-helix surrounding the proline was not severely disrupted (Fig. 2 a). The mK16/K6 backbone proved similar to that of hK16/K6 (Fig. 2 a), with a RMSD of 1.14Å over the entire 1B subdomain (14 heptads), compared with a RMSD of 2.07Å when overlaid with mK17/K6 (Fig. 2 b). RMSD values decreased to 0.68Å when five heptads centered around Pro188 were compared in these dimers, implying that the peptide backbones of the helices are structurally very similar. These modeling efforts nevertheless proved useful in that they exposed an intriguing difference when comparing the side chains of hK16/K6, mK17/K6, and mK16/K6 dimers. In mK17, a hydrophobic stripe of four apolar amino acids, located in b and f positions of consecutive heptad repeats, was exposed to the surface of the dimer, rather than buried within (Fig. 2 c). This hydrophobic stripe spans the region where Pro188 is located in hK16. Moreover, a hydrophilic residue, Gln, replaces one of these hydrophobic residues in mK16 (Fig. 2 d). Otherwise, the hydrophobic stripe is evolutionarily conserved in many type I keratins, including vertebrates and cephalochordates (e.g., Branchiostoma; Fig. 2 e). The hydrophobic stripe is not conserved in any other IF sequence type, including type II keratins (Fig. 2 e).

### The hydrophobic stripe in coil 1B of type I keratins mediates heterotetramer stability

Hydrophobic patches on the surface of proteins are thermodynamically unfavorable in aqueous environments; their presence often is indicative of a region of protein–protein or protein–lipid interaction. In this case, the hydrophobic residues are positioned at a potential interface between two dimers within a keratin tetramer. We postulated that the hydrophobic stripe is important for tetramer stability, and that Pro188 in hK16 would disrupt it by reorienting the side chains of the proximal hydrophobic stripe residues. We designed several mutant proteins that would, according to our postulate, either destabilize

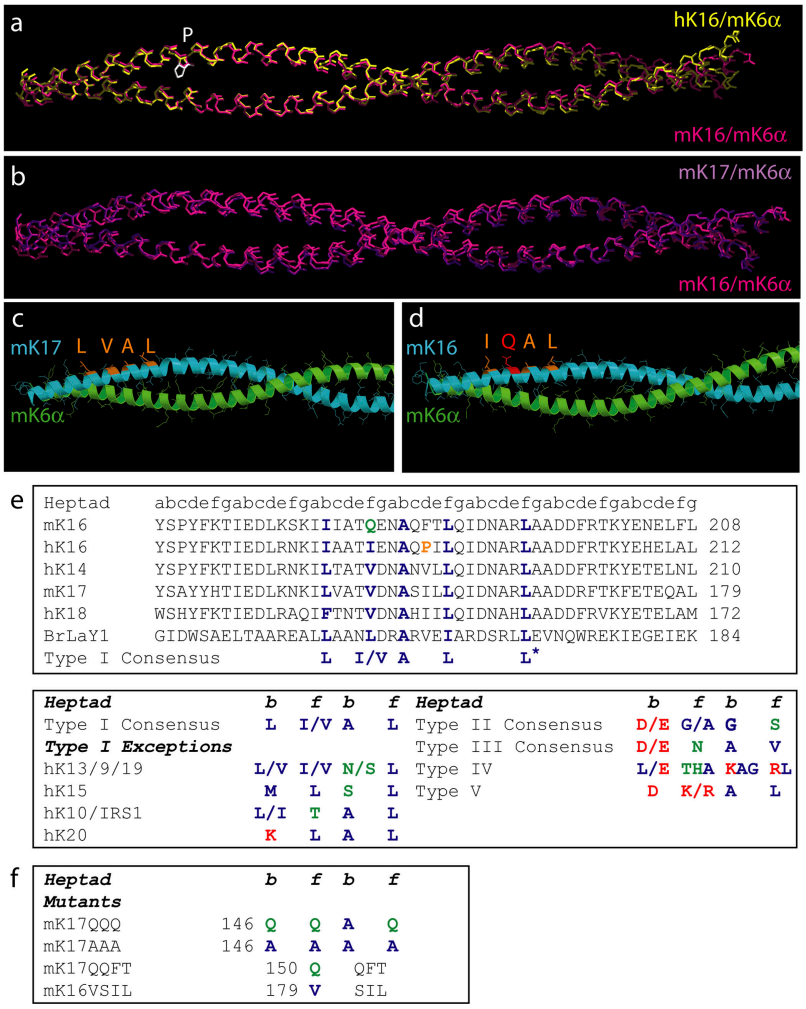


e

| Heptad | abcdefgabcdefgabcdefgabcdefgabcdefgabcdefgabcdefg | |
|---|---|---|
| mK16 | YSPYFKTIEDLKSKIIATQENAQFTLQIDNARLAADDFRTKYENELFL | 208 |
| hK16 | YSPYFKTIEDLRNKIAATIENAQPILQIDNARLAADDFRTKYEHELAL | 212 |
| hK14 | YSPYFKTIEDLRNKILTATVDNANVLLQIDNARLAADDFRTKYETELNL | 210 |
| mK17 | YSAYYHTIEDLKNKILVATVDNASILLQIDNARLAADDRFTKFETEQAL | 179 |
| hK18 | WSHYFKTIEDLRAQIFTNTVDNAHIILQIDNAHLAADDFRVKYETELAM | 172 |
| BrLaY1 | GIDWSAELTAAREALLAANLDRARVEIARDSRLLEVNQWREKIEGEIEK | 184 |
| Type I Consensus | L I/V A L L* | |

| Heptad | b | f | b | f | Heptad | b | f | b | f |
|---|---|---|---|---|---|---|---|---|---|
| Type I Consensus | L | I/V | A | L | Type II Consensus | D/E | G/A | G | S |
| ***Type I Exceptions*** | | | | | Type III Consensus | D/E | N | A | V |
| hK13/9/19 | L/V | I/V | N/S | L | Type IV | L/E | THA | KAG | RL |
| hK15 | M | L | S | L | Type V | D | K/R | A | L |
| hK10/IRS1 | L/I | T | A | L | | | | | |
| hK20 | K | L | A | L | | | | | |

f

| Heptad | | b | f | b | f |
|---|---|---|---|---|---|
| Mutants | | | | | |
| mK17QQQ | 146 | Q | Q | A | Q |
| mK17AAA | 146 | A | A | A | A |
| mK17QQFT | 150 | Q | QFT | | |
| mK16VSIL | 179 | V | SIL | | |

Figure 2. **Type I keratins display a stripe of hydrophobic amino acids on the surface of the type I/type II heterodimer.** Human K16/mK6α, mK17/mK6α, and mK16/mK6α were modeled onto Cortexillin I with Modeller6 (Sali and Blundell, 1993). Figures were generated using POVScript (Fenn et al., 2003) and rendered with Raster3D (Merritt and Bacon, 1997). The carbon backbone coiled-coils were overlaid for comparison. (a) hK16/mK6α (yellow) and mK16/mK6α (pink). (b) mK17/mK6α (purple) and mK16/mK6α (pink). No significant differences in the backbone were observed. (c) mK17 (blue)/K6α (green) dimer. The carbon backbone is represented by the ribbon. The $NH_2$ and COOH termini are left and right, respectively. A stripe of hydrophobic surface residues on K17 are highlighted in orange below their single-letter amino acid codes. (d) mK16 (blue)/K6α (green) dimer. A glutamine residue (red) occurs in the midst of the hydrophobic stripe. (e) Amino acid sequence alignment of type I keratins and consensus sequences of the residues corresponding to the hydrophobic stripe visualized in K17 (see c). The asterisk denotes the presence of an additional hydrophobic, f-position leucine at the COOH terminus of the hydrophobic stripe. Type I consensus sequence is taken from *Branchiostoma Lancelet* type I YI, *Branchiostoma Floridae* type I EI, hK14, hK17, hK18, hK12, and several hard α type I keratins. Consensus sequences for various other IFs (types III–V) are also listed. The heptad repeat (abcdefg) is listed at the top starting from the first amino acid of subdomain 1B. Highlighted residues indicate the positions of the four adjacent hydrophobic amino acids visualized in K17 (see c). Hydrophobic/nonpolar residues (blue), hydrophilic residues (green), and charged residues (red) are colored. Pro 188 in hK16 is coded orange. (f) Four mutant proteins were created, with the mutated amino acids listed below the residues that were changed in each mutant.

mK17-containing tetramers or stabilize mK16-containing tetramers. We mutated three of the four hydrophobic residues in mK17 to Gln (mK17 L146Q, V150Q, L157Q; mutant named mK17QQQ) or Ala (mK17 L146A, V150A, L157A; mutant named mK17AAA; Fig. 2 f). Glutamine was chosen because it is the amino acid found in the midst of mK16's hydrophobic stripe, and it retains the side chain length of the Leu residues it replaces. We chose Ala as a more moderate substitution that maintains the apolar nature of the stripe, but with minimal side chain length. We also swapped four residues between mK16 and mK17 including K16 Q179V and the 3 aa surrounding Pro188 in hK16 (mK16 183QFT to SIL). The reverse was done to K17 (V150Q, 154SIL to QFT). These mutants were designated mK16VSIL and mK17QQFT, respectively (Fig. 2 f).

When assessed by anion exchange chromatography and chemical cross-linking, all three mutant K17/K6 complexes formed unstable tetramers in a similar manner to mK16/K6 (<15% tetramers in 8 M urea). In stark contrast, the mK16VSIL/K6 formed stable tetramers similar to mK17/K6 (>35% tetramers in 8 M urea; Fig. 3, a and b). Of note, mK16 Gln179 (the second amino acid in the hydrophobic stripe; Fig. 2, d and e) is conserved in rat K16 (not depicted). Next, we determined that all mutants formed filaments with the same efficiency as wild-type proteins based on a pelleting assay with high speed centrifugation (Fig. 3 c). Analysis of filament morphology using negative staining and electron microscopy revealed that all mutants formed smooth-surfaced, long filaments that appeared similar to their respective wild-type filaments (Fig. 3, d–g). In particular, the propensity of hK16 (Wawersik et al., 1997) and mK16 (Fig. 3 e) to form small bundles containing two to three filaments was unaltered in mK16VSIL (Fig. 3 g). Thus, the residues forming the hydrophobic stripe on type I keratins are key determinants of the ability to form urea-stable heterotetramers, but do not otherwise significantly affect the potential to form mature filaments in vitro.

## The hydrophobic stripe on type I keratins is accessible on the surface of keratin dimers

We performed binding assays with the hydrophobic-binding fluorophore 8-anilino-1-naphthalenesulfonic acid (ANS), which binds partially folded proteins having small hydrophobic regions exposed to the surface (Semisotnov et al., 1991; Fig. S2, available at http://www.jcb.org/cgi/content/full/jcb.200408116/DC1). Binding of ANS to mK17/K6 heterodimers can reproducibly be detected, and decreases significantly as tetramer formation is allowed to proceed. ANS binding to mK16/K6, mK17AAA/K6, and mK17QQQ/K6 heterodimers is sig-

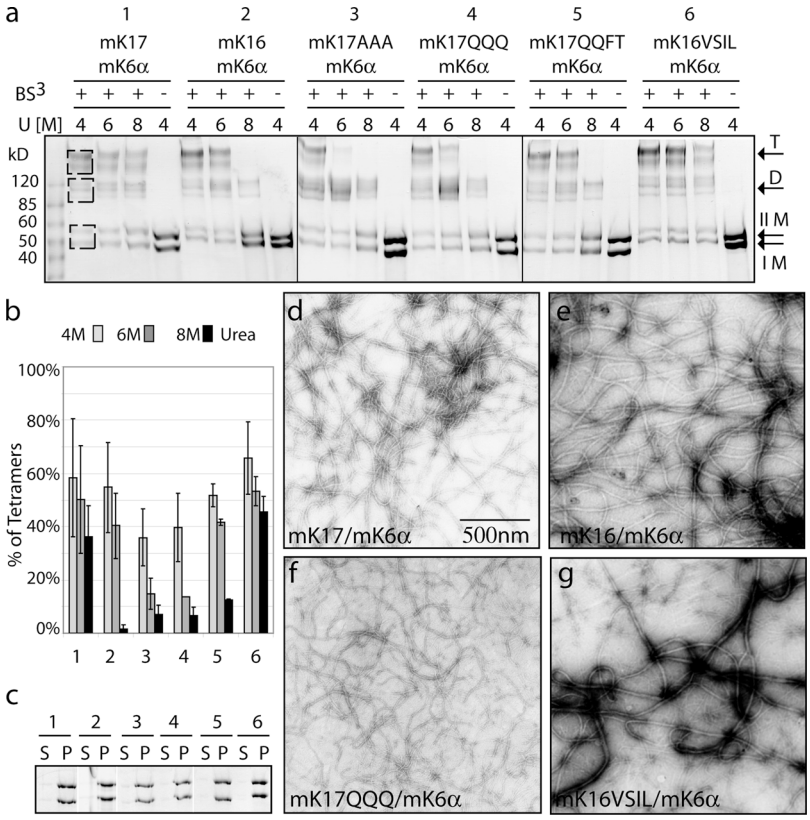


Figure 3. **Mutation of surface hydrophobic residues in type I keratins results in destabilization of tetramers.** (a) Anion-exchange chromatography of types I and II keratin complexes, followed by cross-linking with $BS^3$ in the presence of 4, 6, or 8 M urea was performed as in Fig. 1. Cross-linked products (4 μg of proteins) were analyzed by SDS-PAGE on 4–12% gradient gels. Molecular mass standards are indicated on the left, whereas oligomeric complex positions of tetramer (T), dimer (D) type II (II M) and type I (I M) monomer are indicated on the right. Dashed boxes identify the region quantitated in b. (b) Densitometry was performed on the SDS-PAGE gel in panel a and in replicate experiments. The intensities of monomer, dimer, and tetramer were summed to form 100%, and the percentages of tetramers at 4 M (light gray box), 6 M (dark gray box), or 8 M (black box) urea were graphed (mean ± SEM). (c–g) Heterotypic complexes isolated by anion-exchange chromatography were subjected to standard filament assembly conditions (see Materials and methods). (c) Assembly efficiency was analyzed by a high speed sedimentation assay. Supernatant (S) and pellet (P) were loaded onto an 8.5% polyacrylamide gel, followed by staining with Coomassie blue. White lines indicate that intervening lanes have been spliced out. (d–g) Filaments were negatively stained and visualized with transmission electron microscopy. Type I/type II keratins are listed in the bottom left-hand corner of each image. Bar, 500 nm.

nificantly lesser than to mK17/K6 or mK16VSIL/K6 heterodimers (Fig. S2). ANS binding studies thus provide direct support for the existence of a hydrophobic stripe contributed by type I keratins at the surface of keratin heterodimers, and reveal a tight correlation between binding and ability to form urea-stable tetramers.

### Probing the significance of keratin tetramer stability

We previously showed that K16 could not compete effectively with K14 in the formation of stable heterotypic complexes in the presence of substoichiometric amounts of type II binding partners in vitro (K5 or K6; Paladini et al., 1996). The availability of suitable mouse models created an opportunity to monitor the fate of K16 protein under conditions of limited partner availability (K6 null mice; Wong et al., 2000) or loss of a major type I keratin competitor (K17 null mice; McGowan et al., 2002). Relative to wild-type control, the steady-state levels of K16 protein (but not mRNA) are much decreased in K6 null skin keratinocytes in primary culture, in which K5 is the only type II keratin left and whose protein level does not become elevated (Fig. 4 a; Wong et al., 2000; Wong and Coulombe, 2003). In contrast, the levels of K14 and K17 proteins are not altered in these cells (Wong et al., 2000; Wong and Coulombe, 2003). Conversely, the levels of K16 protein, but not K14, are increased in K17 null keratinocytes compared with control (Fig. 4 a). These data show that in a living cell context in which K5, K6α, K6β, K14, K15, K16, and K17 all coexist, K16 is uniquely sensitive to perturbations of the balance between types I and II keratins.

Lack of a pairing partner causes individual keratins to turn over rapidly in cultured cells (Kulesh et al., 1989; Lersch et al., 1989). Given that tetramer subunits comprise the small soluble pool of cytoplasmic IF proteins (Soellner et al., 1985; Chou et al., 1993), we questioned whether the selective loss of K16 protein (Fig. 4 a) reflected an enhanced turnover rate. [$^{35}$S]Met/Cys pulse-chase experiments performed in K6-null and wild-type keratinocytes showed that K16 protein turned over almost twice as quickly in K6-null compared with wild type (Fig. 4 b). In contrast, K17 protein turnover exhibited no difference between K6-null and wild type (Fig. 4 b). The rate of K14 turnover was slightly enhanced in K6 null compared with wild-type keratinocytes, but less significantly than K16 (Fig. 4 b, 48-h time point). As an additional point, K16 immunoprecipitates showed a lesser amount of type II keratins compared with K14 and K17 immunoprecipitates (Fig. 4 b), suggesting that K16 may be part of smaller heterotypic complexes. K16 was largely excluded from both K14 and K17 immunoprecipitates, whereas sizable amounts of K14 were found in K16 immunoprecipitates (Fig. 4 b). As previously showed, the affinity of K16 for K5 and K6 is practically identical, and the presence of K14 enhances the likelihood of retrieving K16 in urea-stable heterotetramers in vitro (Paladini et al., 1996). Thus, K16 exhibits a faster turnover rate than the related type I keratins K14 and K17 in a physiological context where type II keratin partners are limiting. Also, K16 is recruited into a distinct subset of keratin heterotypic complexes in living cells. It appears likely that the mixing of K14 and K16, but not K17, within the same soluble subunits could play a role in the intermediate half-life exhibited by K14 in K6 null keratinocytes (Fig. 4 b).

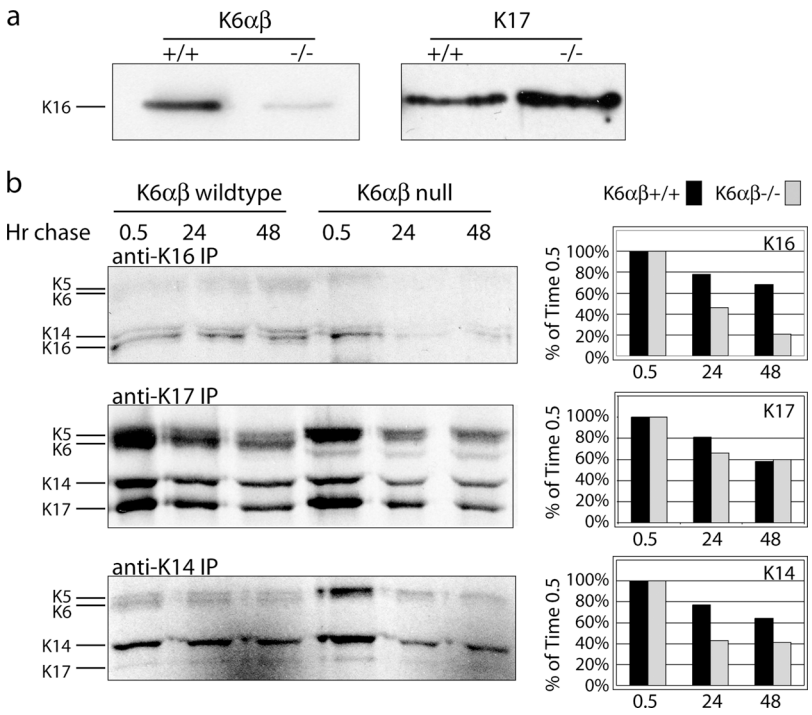


Figure 4. **Keratin 16 protein turns over faster in K6 null keratinocytes than in wild-type keratinocytes.** (a) Primary keratinocytes were isolated from K6 or K17 wild-type and null mice. Equal amounts of protein extract were probed for K16 protein and β-tubulin (not depicted) as a loading control. K16 steady-state protein levels are greatly reduced in K6 null keratinocytes compared with wild-type keratinocytes; whereas K16 steady-state protein levels increase in K17 null keratinocytes. (b) Primary keratinocytes were isolated from K6 wild-type and null mice and pulse-chased with [$^{35}$S]Met/Cys. Equal amounts of cell lysates were immunoprecipitated with antibodies against K16, K17, or K14. Immunoprecipitation was repeated two times to ensure maximal extraction of both labeled and unlabeled protein. Equal amounts of immunoprecipitated samples were separated via SDS-PAGE and autoradiographed. Complexes of keratins were pulled down in the immunoprecipitation; keratins are identified at the left, whereas the immunoprecipitating antibody is indicated above each autoradiograph. Autoradiographs were quantitated by densitometry. Bar graphs to the right show the percentage of label remaining at the various time points. K6αβ +/+ (black box) and K6αβ −/− (gray box).

## Discussion

### Differential keratin tetramer stability and its potential significance in vivo

The ability to obtain high yields of type I/II keratin heterotetramers in the presence of 8 M urea underscores the unusual stability of these complexes, and hints at a key role for hydrophobic interactions during their formation. We identified a novel determinant–a short stripe of four hydrophobic residues aligned on the surface of coil 1B in type I keratins engaged in heterodimers–that underlies this property. This stripe is specific to type I keratins capable of forming urea-stable heterotetramers, such as K14, K17 (Wawersik et al., 1997) and K18 (Yamada et al., 2002), and is imperfectly conserved in K19 (Fradette et al., 1998), K10 (unpublished data), and K16 (Wawersik et al., 1997; this study), all unable to form urea-stable tetramers. Three different assays (anion exchange chromatography, cross-linking, and blue native gel electrophoresis) have shown consistently that K16 forms less stable tetramers than related type I keratins. For mK16, this property is likely due to the discontinuity of the hydrophobic stripe in coil 1B. The duplication of these observations with both purified, recombinant proteins in vitro and native keratin complexes in the context of total protein lysates from cultured primary keratinocytes supports a likely physiological role for this newly defined determinant. The ability to interconvert between urea-stable and urea-unstable heterotetramers through site-directed mutagenesis suggests that this hydrophobic stripe is a key determinant of the differential stability of keratin tetramers under denaturing conditions. Other IFs, including the type III vimentin, are missing this stripe, correlating with the inability of vimentin to form stable tetramers in 6 M urea (Coulombe and Fuchs, 1990). Given that in vitro assembly buffer conditions differ between IF types, it is likely that the driving forces for tetramerization (and further assembly) also differ between IF types. Our report extends others focused on the role of charged residues (Meng et al., 1994; Mehrani et al., 2001), which are periodically distributed in the rod domain (Parry et al., 1977; McLachlan and Stewart, 1982). Charge interactions that strongly influence keratin tetramer stability (without disrupting filament formation) in vitro have been identified in coils 1A, 2A, and 2B, but not in coil 1B (Mehrani et al., 2001). Also, charge interactions between the relatively basic rod-proximal head domain and the relatively acidic rod domain have been shown to influence tetramerization (Hatzfeld and Burba, 1994; Mucke et al., 2004). Comparison of the presence of hydrophobic stripe identified in this work with other hydrophobic and charged residues in the 1B domain reveals an overall negative charge on the COOH-terminal portion of the 1B domain, a more negative charge on the $NH_2$-terminal portion, with the hydrophobic stripe present near the junction of these two domains (Fig. 5, a–d). Here, we provide data that hydrophobic interactions in subdomain 1B are a contributing force in stabilizing keratin tetramers.

Remarkably, distinct amino acids located at discrete positions of coil 1B in human and mouse K16 underlie the formation of less stable tetramers in vitro, raising the prospect of convergent evolution. As further support, the proline residue in human K16 is conserved in both chimp (Acc# XP_511810) and dog K16 (Acc# XP_548101) such that all K16 sequences known to date contain either the proline residue (human, chimp, and dog K16) or an incomplete hydrophobic stripe (rat and mouse K16). A priori, the presence of Pro188 in a "d" position of the heptad repeat in hK16 (normally buried in the coiled-coil hydrophobic core) is at odds with the proposed role for the surface-exposed hydrophobic stripe. We suggest that this Pro residue, which occurs between the third and fourth hy-

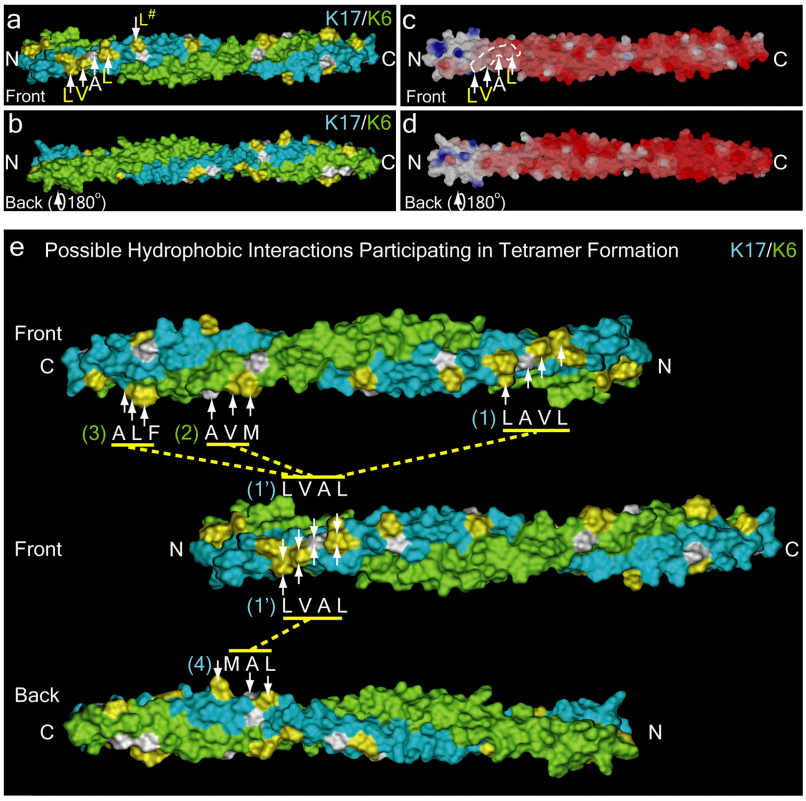


Figure 5. **Modeling hydrophobic interactions leading to keratin tetramer formation and/or stability.** (a) Surface contour of the modeled K17 (blue)/K6α (green) heterodimer. Hydrophobic residues are highlighted in yellow; alanine residues are white. Arrows point to the main hydrophobic stripe. As shown in Fig. 2 e, an additional f-position leucine (#) may be part of the main hydrophobic stripe. (b) Same as a, except the model has been flipped 180° along a horizontal axis to show the back side of the coiled-coil. (c and d) Electrostatic surface contour of the K17/K6α heterodimer. The hydrophobic stripe is outlined with dashes. Negative charges are depicted by red; positive charges are depicted by blue. (e) Potential interactions between the main hydrophobic stripe and other shorter stripes present in the 1B domain of both types I and II keratins are depicted by dotted lines between two adjacent dimers. The face of interaction between two dimers within a tetramer is unknown. Also, it is unknown whether two dimers supercoil around each other, or exist as straight coils (Er Rafik et al., 2004). Depending on the axial alignment of antiparallel dimers, the hydrophobic stripe may interact with self (1—1′) or with the shorter strips (1—2, 1—3, 1—4). Because the azimuthal alignment is also unknown, the top and bottom models depict front and back views of the same dimer, oriented in the same direction (C–N), so that all hydrophobic stripes and potential tetrameric interactions can be viewed. The three dimers shown are not to be confused as a potential hexamer; rather the image shows two views of the same tetramer, with the central dimer present in both views. To simplify, we have depicted interactions with only the main hydrophobic stripe in the central dimer (1′). Additional interactions could occur between the shorter stripes 2′, 3′, and 4′ (not depicted) in the center dimer and those already denoted in the top and bottom dimers.

drophobic amino acids in the hydrophobic stripe (Fig. 2, a and e), disturbs the local α-helical backbone (as supported by modeling), altering side chain angles in proximal amino acids and in the end, misaligning the surface hydrophobes that normally stabilize keratin dimer–dimer interactions. Such side chain reorientation can occur in the context of a coiled coil, as previously shown for myosin (Li et al., 2003). The spatial orientation of hydrophobic side-chains within the stripe is likely important in determining their availability for mediating interactions between keratin heterodimers (Er Rafik et al., 2004).

The paucity of knowledge regarding IF assembly in vivo complicates the determination of the significance of differential tetramer stability, observed in an artificial setting in vitro. By the criteria of mild detergent extraction and high speed centrifugation, the soluble pool of IFs in the cytoplasm is small (<1% in keratinocytes) and consists mostly of tetramers (Soellner et al., 1985; Chou et al., 1993). The amount of hK16 retrieved from the soluble pool does not increase when overexpressed in transgenic mouse skin (Paladini and Coulombe, 1999), suggesting that Pro188 does not affect partitioning to the "soluble pool" in living keratinocytes. Tetramer instability could, as shown here, influence protein half-life under specific circumstances defined in part by assembly partner availability. Another possible outcome is an influence on the size or composition of keratin heterotetramers. Our studies in skin keratinocytes in primary culture revealed at least two types of keratin complexes: those rich in K14 and K17; and those rich in K14 and K16 (Fig. 4 b, 0.5-h time point). Monomeric composition can influence the micromechanical properties of keratin filaments in vitro (Yamada et al., 2002). The physiological relevance of these and other possibilities can be addressed in future studies.

## Implications for the structure of the polymerization-competent IF tetramer

The discovery of the hydrophobic stripe in the coil 1B domain of type I keratins creates an obvious question: To what does it bind as antiparallel dimers dock alongside one another to form the tetramer? In the answer lies key insight into the axial alignment of antiparallel dimers within the keratin tetramer subunit. Substoichiometric cross-linking of large oligomers of either type I/II or type III IF proteins identified several tetramer conformations by "nearest neighbor analyses" (Geisler et al., 1992; Steinert et al., 1993a,b,c; Mucke et al., 2004). A recent study (Hess et al., 2004) in which site-directed spin labeling and electron paramagnetic resonance (EPR) were used to analyze the interactions occurring as vimentin transitions from a monomeric state to large oligomers in vitro provided direct, site-specific evidence that the $A_{11}$ intermediate, which places coil 1B of antiparallel dimers en face, corresponds to the earliest tetramer intermediate. The $A_{22}$ conformation, which places coil 2B of antiparallel dimers en face, occurs concomitant with the formation of larger oligomers (Hess et al., 2004). On one hand, the EPR findings of Hess et al. (2004) yield spatial constraints that are not compatible with the hydrophobic stripe interacting with self in the context of a keratin $A_{11}$ tetramer. On the other hand, comparative studies based on cross-linking (Steinert et al., 1993c) and mass-per-unit length determination (Herrmann et al., 1999) yielded strong evidence that precise axial stagger of antiparallel dimers differs for keratin and vimentin tetramers.

Higher resolution analyses are needed to identify the site(s) interacting with the newly defined hydrophobic stripe on type I keratins, and the resulting structure of the keratin tetramer subunit. There are ~20 hydrophobic amino acids in coil 1B domain of both types I and II keratins that are not in "a" or "d" heptad positions, and potentially exposed to the surface of the dimer. Short stripes of less than three hydrophobic amino acids exist in the COOH-terminal half of coil 1B in both types I and II keratins (Fig. 5 e) which, depending on their orientation in space, could interact with the hydrophobic stripe identified in the $NH_2$-terminal half of 1B. Whether coiled-coil dimers are supercoiled within tetramers or not (Er Rafik et al., 2004) is an important consideration. As an additional possibility, the hydrophobic stripe could sequentially interact with multiple regions within coil 1B through "axial slippage", which is believed to occur in several instances. For example, as part of conformational changes within a filament as it reaches its final, most energetically stable structure (Mucke et al., 2004), in response to mechanical stretching (Kreplak et al., 2002) or association with other filaments or interacting proteins (Aebi et al., 1988), or as the basis for the IF-dependent mechanotransduction of signals (Mucke et al., 2004).

## Materials and methods

**Plasmid generation**

The following constructs were used: pET-hK14 (Coulombe and Fuchs, 1990), pET-hK16, pET-hK6b (Paladini et al., 1996), pET-mK16b (Bernot et al., 2002). The pET-mK17, pET-mK6α, pET-mK6β plasmids were created by subcloning (New England Biolabs, Inc.) the relevant cDNA (McGowan and Coulombe, 1998) into pET-3d (Studier et al., 1990). The QuickChange Site-Specific Mutagenesis kit (Stratagene) was used on the pET-mK17 and the pET-mK16 plasmids with the following sense primers to create the designated mutants (underlined residues are mutant compared with the wild-type sequence): mK17QQQ: 5′-GGATCTGAAGAACAAGATCCAAGTGGCCACCCAGGACAATGCTAGCATCCTGCAGCAGATTGACAATGCTCGTCTGGC-3′; mK17AAA: 5′-GGATCTGAAGAACAAGATCGCTGTGGCCACCGCGGACAATGCTAGCATCCTGGCCCAGATTGACAATGCTCGTCTGGC-3′; mK17QQFT:5′-CCTTGTGGCCACCCAGGACAATGCCCAGTTCACGCTGCAGATTGACAATGCTCGTCTGGC-3′ and mK16VSIL: 5′-GCAAGATCATTATTGCCACCGTGGAGAATGCATCGATCCTTCTGCAGATTGACAATGCCAGGC-3′.

**Recombinant protein purification, anion exchange chromatography, and cross-linking assay**

pET plasmids were transformed into BL21(DE3) *E. coli* for recombinant protein expression. Proteins were extracted from inclusion bodies (Paladini et al., 1996) and solubilized in buffer A containing 6.5 M urea, 50 mM Tris-HCl, pH 8.0, 1 mM EGTA, 2 mM DTT, and 30 μg/ml PMSF. Proteins were purified to near homogeneity via anion exchange chromatography with a High-Trap Q column (Amersham Biosciences; Wawersik et al., 1997). Purified types I and II keratins (0.5 mg/ml) were mixed (45:55 M ratio) for 1 h, loaded onto a Mono Q column (Amersham Biosciences), and eluted with linear gradients of 0–125 mM and 125–300 mM guanidine-HCl in buffer A (Coulombe and Fuchs, 1990; Wawersik et al., 1997). Fractions were analyzed by SDS-PAGE. Heterotypic complexes (200 μg/ml) containing types I and II keratin in a 1:1 M ratio were dialyzed overnight into 25 mM sodium-phosphate buffer, pH 7.4, containing 4, 6, 6.5, 8, or 9 M urea plus 10 mM β-mercaptoethanol. The cross-linker $BS^3$ (Pierce Chemical Co.) was added for 1 h, and products analyzed by SDS-PAGE and gel scanning densitometry.

**Blue native gel electrophoresis**

A detailed description of blue native gel electrophoresis was provided previously (Schagger, 2001). Primary keratinocytes were cultured and lysed with 8 M or 6 M urea in buffer A (see above). After centrifugation to remove debris, 10 μg lysate was mixed with 5% Coomassie G250 in 500 mM 6-aminohexanoic acid and loaded onto a 5–13% acrylamide gradient gel (48 acrylamide:1.5 bisacrylamide; 25 mM imidazole; 500 mM 6-aminohexanoic acid). After gel electrophoresis, the protein was then transferred onto PVDF membrane (Bio-Rad Laboratories), destained in 30% methanol, 10% acetic acid), and conventional Western analysis was performed.

**Filament assembly and pelleting assay**

Heterotypic complexes (200 μg/ml) obtained from Mono Q fractionation were denatured in 9 M urea, 1 mM DTT, 25 mM Tris-HCl, pH 7.5, for 4 h. Keratin polymerization was induced by dialysis in 5 mM Tris-HCl, pH 7.5, 1 mM DTT, containing 4 M urea (2 h), 2 M urea (2 h), then no urea for >2 h, all at RT. Polymerized filaments were viewed by negative staining (1% uranyl acetate) on a carbon-coated 400 mesh grid (Ted Pella) with a transmission electron microscope (model CM120; Philips) operated at 60 kV. For the pelleting assay, 50 μl of assembled filaments (~10 μg protein) was subjected to centrifugation in an airfuge at 28 psi for 30 min. The supernatant and pellet were analyzed by SDS-PAGE and gel-scanning densitometry.

**Modeling keratin 1B dimers**

The crystal structure of Cortexillin I (PCB 1D7M) was chosen as a template for the coiled coil 1B dimer. Alignment of Cortexillin I, vimentin, and keratin sequences was performed using default parameters by CLUSTALX (Thompson et al., 1997). Homology model building was performed using the default parameters for energy minimization of Modeller6 (Sali and Blundell, 1993). No further energy minimization was performed. After a minimum of 10 model-building runs, models of individual keratin heterodimers or vimentin homodimers were almost identical. Models with the lowest energy states were chosen for further analysis. Manual inspection was performed using the Swiss pdb viewer (Guex and Peitsch, 1997), and further evaluation was performed through analyses of 3D profiles (Eisenberg method), atomic interactions (ERRAT), and Ramachandran plots (PROCHECK, all available at UCLA-DOE Institute for Genomics and Proteomics, http://www.doe-mbi.ucla.edu/Services/SV/). Variability was assessed by superimposing C-α traces and backbones of select models onto the template and calculating RMSD values for positional differences between equivalent atoms. The protein structures were visualized and analyzed on MolMol (Koradi et al., 1996).

**Pulse-chase labeling experiments and immunoprecipitations**

Skin keratinocytes were isolated from 3-d-old 129SvJ wild-type or $K6^{-/-}$ (Wong et al., 2000) pups and seeded in primary culture in 35- or 60-mm tissue culture plates. After 3 d, or when the plates were 90% confluent, cells were starved with DME medium lacking Met and Cys for 30 min. Cells were then pulse labeled with 0.1 mCi/ml [$^{35}$S]Met/Cys (Easy Tag Express Protein Labeling Mix; PerkinElmer) for 20 min. After washing the cells with PBS, labeled cells were chased with normal mKer medium. After 0, 24, or 48 h, the cells were washed and collected in the presence of protease inhibitors, and stored (–80°C). For immunoprecipitation, cells were solubilized with 2% Empigen BB (Calbiochem) in PBS supplemented with 5 mM EDTA and protease inhibitors. Lysates were analyzed by SDS-PAGE and Western blotting for actin (AC40; Sigma-Aldrich) or β-tubulin (DM1A; Sigma-Aldrich). Protein A Sepharose beads (Amersham Biosciences) were washed with PBS and then bound to rabbit polyclonal antibodies directed against K16 (Bernot et al., 2002), K17 (McGowan and Coulombe, 1998), and K14 (AF 64; Covance). Equal protein amounts from lysates (based on actin or β-tubulin load) were added to conjugated beads and incubated overnight at 4°C. Beads were washed with 0.2% Empigen BB. Bound protein was eluted with 5× gel sample buffer containing β-mercaptoethanol. A second immunoprecipitation was performed on the same lysate to ensure complete epitope(s) depletion. Eluted proteins were subjected to SDS-PAGE and Coomassie staining. The gel was incubated for 20 min in ENLIGHTENING autoradiography enhancer (PerkinElmer), dried, and exposed to BiomaxMR film (Kodak), and analyzed by densitometry.

**Online supplemental material**

Online supplemental material includes the generation of chimeric proteins in which the 1B subdomain between K17 and K16 has been swapped as well as anion exchange chromatography and cross-linking data obtained using these chimeras (Fig. S1). Also shown is spectroscopy analysis of ANS binding to wild-type and mutant dimers (Fig. S2), which provides direct support for the existence of a hydrophobic stripe contributed by type I keratins at the surface of keratin heterodimers. Online supplemen-

tal material is available at http://www.jcb.org/cgi/content/full/jcb.200408116/DC1.

We thank Dr. David Shortle for advice and thank Dr. Matthew Wawersik for his generous help.

This work was supported by grants AR44232 and AR42047 from the National Institutes of Health to P.A. Coulombe.

Submitted: 20 August 2004
Accepted: 28 January 2005

## References

Aebi, U., M. Haner, J. Troncoso, R. Eichner, and A. Engel. 1988. Unifying principles in intermediate filament assembly. *Protoplasma.* 145:73–81.

Bernot, K.M., P.A. Coulombe, and K.M. McGowan. 2002. Keratin 16 expression defines a subset of epithelial cells during skin morphogenesis and the hair cycle. *J. Invest. Dermatol.* 119:1137–1149.

Briki, F., J. Doucet, and C. Etchebest. 2002. A procedure for refining a coiled coil protein structure using x-ray fiber diffraction and modeling. *Biophys. J.* 83:1774–1783.

Burkhard, P., R.A. Kammerer, M.O. Steinmetz, G.P. Bourenkov, and U. Aebi. 2000. The coiled-coil trigger site of the rod domain of cortexillin I unveils a distinct network of interhelical and intrahelical salt bridges. *Struct. Fold. Des.* 8:223–230.

Chou, C.F., C.L. Riopel, L.S. Rott, and M.B. Omary. 1993. A significant soluble keratin fraction in "simple" epithelial cells. Lack of an apparent phosphorylation and glycosylation role in keratin solubility. *J. Cell Sci.* 105:433–445.

Cohen, C., and D.A. Parry. 1990. Alpha-helical coiled coils and bundles: how to design an alpha-helical protein. *Proteins.* 7:1–15.

Coulombe, P.A., and E. Fuchs. 1990. Elucidating the early stages of keratin filament assembly. *J. Cell Biol.* 111:153–169.

Coulombe, P.A., and M.B. Omary. 2002. Hard and soft principles defining the structure, function and regulation of keratin intermediate filaments. *Curr. Opin. Cell Biol.* 14:110–122.

Coulombe, P.A., and P. Wong. 2004. Cytoplasmic intermediate filaments revealed as dynamic and multipurpose scaffolds. *Nat. Cell Biol.* 6:699–706.

Crick, F.H. 1952. Is alpha-keratin a coiled coil? *Nature.* 170:882–883.

Er Rafik, M., J. Doucet, and F. Briki. 2004. The intermediate filament architecture as determined by X-ray diffraction modeling of hard alpha-keratin. *Biophys. J.* 86:3893–3904.

Fenn, T.D., D. Ringe, and G.A. Petsko. 2003. POVScript+: a program for model and data visualization using persistence of vision ray-tracing. *J. Appl. Crystallogr.* 36:944–947.

Fradette, J., L. Germain, P. Sessaiah, and P.A. Coulombe. 1998. The type I keratin 19 possesses distinct and context-dependent assembly properties. *J. Biol. Chem.* 273:35176–35184.

Fuchs E., and D.W. Cleveland. 1998. A structural scaffolding of intermediate filaments in health and disease. *Science*. 279:514–519.

Geisler, N., J. Schunemann, and K. Weber. 1992. Chemical cross-linking indicates a staggered and antiparallel protofilament of desmin intermediate filaments and characterizes one higher-level complex between protofilaments. *Eur. J. Biochem.* 206:841–852.

Guex, N., and M.C. Peitsch. 1997. SWISS-MODEL and the Swiss-PdbViewer: an environment for comparative protein modeling. *Electrophoresis.* 18: 2714–2723.

Hatzfeld, M., and M. Burba. 1994. Function of type I and type II keratin head domains: their role in dimer, tetramer and filament formation. *J. Cell Sci.* 107:1959–1972.

Herrmann, H., and U. Aebi. 1998. Intermediate filament assembly: fibrillogenesis is driven by decisive dimer-dimer interactions. *Curr. Opin. Struct. Biol.* 8:177–185.

Herrmann, H., M. Haner, M. Brettel, N.O. Ku, and U. Aebi. 1999. Characterization of distinct early assembly units of different intermediate filament proteins. *J. Mol. Biol.* 286:1403–1420.

Hess, J.F., M.S. Budamagunta, J.C. Voss, and P.G. FitzGerald. 2004. Structural characterization of human vimentin rod 1 and the sequencing of assembly steps in intermediate filament formation in vitro using SDSL and EPR. *J. Biol. Chem.* 279:44841–44846.

Hess, J.F., J.C. Voss, and P.G. FitzGerald. 2002. Real-time observation of coiled-coil domains and subunit assembly in intermediate filaments. *J. Biol. Chem.* 277:35516–35522.

Hesse, M., T.M. Magin, and K. Weber. 2001. Genes for intermediate filament proteins and the draft sequence of the human genome: novel keratin genes and a surprisingly high number of pseudogenes related to keratin genes 8 and 18. *J. Cell Sci.* 114:2569–2575.

Janmey, P.A. 1991. Mechanical properties of cytoskeletal polymers. *Curr. Opin. Cell Biol.* 3:4–11.

Koradi, R., M. Billeter, and K. Wuthrich. 1996. MOLMOL: a program for display and analysis of macromolecular structures. *J. Mol. Graph.* 14:51–55, 29-32.

Kreplak, L., A. Franbourg, F. Briki, F. Leroy, D. Dalle, and J. Doucet. 2002. A new deformation model of hard alpha-keratin fibers at the nanometer scale: implications for hard alpha-keratin intermediate filament mechanical properties. *Biophys. J.* 82:2265–2274.

Kulesh, D.A., G. Cecena, Y.M. Darmon, M. Vasseur, and R.G. Oshima. 1989. Posttranslational regulation of keratins: degradation of mouse and human keratins 18 and 8. *Mol. Cell. Biol.* 9:1553–1565.

Lersch, R., V. Stellmach, C. Stocks, G. Giudice, and E. Fuchs. 1989. Isolation, sequence, and expression of a human keratin K5 gene: transcriptional regulation of keratins and insights into pairwise control. *Mol. Cell. Biol.* 9:3685–3697.

Li, Y., J.H. Brown, L. Reshetnikova, A. Blazsek, L. Farkas, L. Nyitray, and C. Cohen. 2003. Visualization of an unstable coiled coil from the scallop myosin rod. *Nature.* 424:341–345.

McGowan, K.M., and P.A. Coulombe. 1998. Onset of keratin 17 expression coincides with the definition of major epithelial lineages during skin development. *J. Cell Biol.* 143:469–486.

McGowan, K.M., X. Tong, E. Colucci-Guyon, F. Langa, C. Babinet, and P.A. Coulombe. 2002. Keratin 17 null mice exhibit age- and strain-dependent alopecia. *Genes Dev.* 16:1412–1422.

McLachlan, A.D., and M. Stewart. 1982. Periodic charge distribution in the intermediate filament proteins desmin and vimentin. *J. Mol. Biol.* 162: 693–698.

Mehrani, T., K.C. Wu, M.I. Morasso, J.T. Bryan, L.N. Marekov, D.A. Parry, and P.M. Steinert. 2001. Residues in the 1A rod domain segment and the linker L2 are required for stabilizing the A11 molecular alignment mode in keratin intermediate filaments. *J. Biol. Chem.* 276:2088–2097.

Meng, J.J., S. Khan, and W. Ip. 1994. Charge interactions in the rod domain drive formation of tetramers during intermediate filament assembly. *J. Biol. Chem.* 269:18679–18685.

Merritt, E.A., and D.J. Bacon. 1997. Raster3D: photorealistic molecular graphics in enzymology. *Methods Enzymol.* 277:505–524.

Mucke, N., T. Wedig, A. Burer, L.N. Marekov, P.M. Steinert, J. Langowski, U. Aebi, and H. Herrmann. 2004. Molecular and biophysical characterization of assembly-starter units of human vimentin. *J. Mol. Biol.* 340:97–114.

Omary, M.B., P.A. Coulombe, and I.M. McLean. 2004. Intermediate filament proteins and their associated diseases. *N. Engl. J. Med.* 351:2087–2100.

Paladini, R.D., and P.A. Coulombe. 1999. The functional diversity of epidermal keratins revealed by the partial rescue of the keratin 14 null phenotype by keratin 16. *J. Cell Biol.* 146:1185–1201.

Paladini, R.D., K. Takahashi, N.S. Bravo, and P.A. Coulombe. 1996. Onset of re-epithelialization after skin injury correlates with a reorganization of keratin filaments in wound edge keratinocytes: defining a potential role for keratin 16. *J. Cell Biol.* 132:381–397.

Parry, D.A., W.G. Crewther, R.D. Fraser, and T.P. MacRae. 1977. Structure of alpha-keratin: structural implication of the amino acid sequences of the type I and type II chain segments. *J. Mol. Biol.* 113:449–454.

Parry, D.A., and P.M. Steinert. 1999. Intermediate filaments: molecular architecture, assembly, dynamics and polymorphism. *Q. Rev. Biophys.* 32:99–187.

Porter, R.M., A.M. Hutcheson, E.L. Rugg, R.A. Quinlan, and E.B. Lane. 1998. cDNA cloning, expression, and assembly characteristics of mouse keratin 16. *J. Biol. Chem.* 273:32265–32272.

Quinlan, R.A., J.A. Cohlberg, D.L. Schiller, M. Hatzfeld, and W.W. Franke. 1984. Heterotypic tetramer (A2D2) complexes of non-epidermal keratins isolated from cytoskeletons of rat hepatocytes and hepatoma cells. *J. Mol. Biol.* 178:365–388.

Sali, A., and T.L. Blundell. 1993. Comparative protein modelling by satisfaction of spatial restraints. *J. Mol. Biol.* 234:779–815.

Schagger, H. 2001. Blue-native gels to isolate protein complexes from mitochondria. *Methods Cell Biol.* 65:231–244.

Semisotnov, G.V., N.A. Rodionova, O.I. Razgulyaev, V.N. Uversky, A.F. Gripas, and R.I. Gilmanshin. 1991. Study of the "molten globule" intermediate state in protein folding by a hydrophobic fluorescent probe. *Biopolymers.* 31:119–128.

Soellner, P., R.A. Quinlan, and W.W. Franke. 1985. Identification of a distinct

soluble subunit of an intermediate filament protein: tetrameric vimentin from living cells. *Proc. Natl. Acad. Sci. USA.* 82:7929–7933.

Steinert, P.M. 1991. Analysis of the mechanism of assembly of mouse keratin 1/keratin 10 intermediate filaments in vitro suggests that intermediate filaments are built from multiple oligomeric units rather than a unique tetrameric building block. *J. Struct. Biol.* 107:175–188.

Steinert, P.M., L.N. Marekov, R.D. Fraser, and D.A. Parry. 1993a. Keratin intermediate filament structure. Crosslinking studies yield quantitative information on molecular dimensions and mechanism of assembly. *J. Mol. Biol.* 230:436–452.

Steinert, P.M., L.N. Marekov, and D.A. Parry. 1993b. Conservation of the structure of keratin intermediate filaments: molecular mechanism by which different keratin molecules integrate into preexisting keratin intermediate filaments during differentiation. *Biochemistry.* 32:10046–10056.

Steinert, P.M., L.N. Marekov, and D.A. Parry. 1993c. Diversity of intermediate filament structure. Evidence that the alignment of coiled-coil molecules in vimentin is different from that in keratin intermediate filaments. *J. Biol. Chem.* 268:24916–24925.

Strelkov, S.V., H. Herrmann, and U. Aebi. 2003. Molecular architecture of intermediate filaments. *Bioessays.* 25:243–251.

Strelkov, S.V., H. Herrmann, N. Geisler, A. Lustig, S. Ivaninskii, R. Zimbelmann, P. Burkhard, and U. Aebi. 2001. Divide-and-conquer crystallographic approach towards an atomic structure of intermediate filaments. *J. Mol. Biol.* 306:773–781.

Studier, F.W., A.H. Rosenberg, J.J. Dunn, and J.W. Dubendorff. 1990. Use of T7 RNA polymerase to direct expression of cloned genes. *Methods Enzymol.* 185:60–89.

Thompson, J.D., T.J. Gibson, F. Plewniak, F. Jeanmougin, and D.G. Higgins. 1997. The CLUSTAL_X windows interface: flexible strategies for multiple sequence alignment aided by quality analysis tools. *Nucleic Acids Res.* 25:4876–4882.

Wawersik, M., R.D. Paladini, E. Noensie, and P.A. Coulombe. 1997. A proline residue in the a-helical rod domain of type I keratin 16 destabilizes keratin heterotetramers and influences incorporation into filaments. *J. Biol. Chem.* 272:32557–32565.

Wong, P., E. Colucci-Guyon, K. Takahashi, C. Gu, C. Babinet, and P.A. Coulombe. 2000. Introducing a null mutation in the mouse K6alpha and K6beta genes reveals their essential structural role in the oral mucosa. *J. Cell Biol.* 150:921–928.

Wong, P., and P.A. Coulombe. 2003. Loss of keratin 6 (K6) proteins reveals a function for intermediate filaments during wound repair. *J. Cell Biol.* 163:327–337.

Yamada, S., D. Wirtz, and P.A. Coulombe. 2002. Pairwise assembly determines the intrinsic potential for self-organization and mechanical properties of keratin filaments. *Mol. Biol. Cell.* 13:382–391.